Hindawi
Advances in Polymer Technology
Volume 2020, Article ID 8946591, 10 pages
https://doi.org/10.1155/2020/8946591

*Research Article*

# Tensile Behavior of Acrylonitrile Butadiene Styrene at Different Temperatures

**Jiquan Li**,[1] **Yadong Jia**,[1] **Taidong Li**,[1] **Zhou Zhu**,[1] **Hangchao Zhou**,[2] **Xiang Peng**,[1] **and Shaofei Jiang**[1]

[1]*Key Laboratory of E&M, Ministry of Education, Zhejiang University of Technology, Hangzhou 310014, China*
[2]*Mechanical Light Industry Inspection Department, Zhejiang Fangyuan Test Group Co., Ltd, Hangzhou 310018, China*

Correspondence should be addressed to Shaofei Jiang; jsf75@zjut.edu.cn

Received 30 July 2019; Accepted 15 November 2019; Published 4 April 2020

Guest Editor: Yun Zhang



Temperature greatly influences the mechanical response of acrylonitrile butadiene styrene (ABS). The tensile behavior of ABS was explored in this study. The tensile experiments were conducted at a wide range of temperatures (from 40°C to 130°C). A model was established to reveal the quantitative relationship between temperature and tensile behavior of ABS. The results of tensile experiments showed that tensile behavior of ABS exhibited glassy state and high-elastics state. The model was also divided into two parts that rely on the boundary of glass transition temperature, in which the parameters of the model were calculated by the fitting method. The model predictions showed a good agreement with the results of the experimental tensile test. This study provides the quantitative relationship between temperature and tensile behavior of ABS, which saves time and experimental costs.

## 1. Introduction

Mechanical behavior of amorphous polymers has been studied for many decades, and the basic features of the stress-strain curves are well known [1–3]. At very small strains, the behavior is elastic. At slightly larger strains, yielding occurs when intermolecular barriers to segmental rearrangements are overcome. Following yielding, strain softening may happen, which means a reduction in stress to a level corresponding to plastic flow [4, 5]. Due to their light weight and excellent mechanical properties, amorphous polymers are widely used in automotive industries [6], packaging applications [7], and electronic products [8].

The complex mechanical behavior of amorphous polymers is generally temperature dependent [3, 9, 10]. Over the years, many models have been proposed for the determination of relationship between temperature, stress, and strain [11–13]. Richeton et al. [14] carried out uniaxial compression stress-strain tests at a wide range of temperatures (−40°C to 180°C) to study the influence of temperature on the mechanical behavior of three amorphous polymers. Blumenthal et al. [15] examined the influence of both strain rate and temperature on the deformation response of PMMA and PC. Cady et al. [16] studied the mechanical response of several polymers under dynamic loading at high temperatures. The aforementioned studies resulted in guidelines of how to construct tailored materials, which could serve our needs of improved materials without the need of extensive trial and error work [17].

ABS is an important component of amorphous polymers, especially in the electronics industry, machinery industry, transportation, and building materials industry. [18, 19]. According to the latest report released by Global Market Insights [20], ABS market sales will increase to $38 billion in 2024, with a compound annual growth rate of 6.0%. The potential growth of household appliances, electronic appliances, automobiles, and construction industry will promote the rapid development of ABS market. Thus, the use of ABS has become commonplace.

However, the influence of temperature on the tensile behavior of ABS has received much less attention. The purpose of this work is to propose a mathematical model for

describing tensile behavior of ABS at different temperatures (from 40°C to 130°C), in which the parameters of the model were calculated by a fitting method. To verify the accuracy of the model, the prediction results from the model were compared with the experimental results. This study provides the quantitative relationship between temperature and tensile behavior of ABS, which saves time and experimental costs.

## 2. Modeling

The amorphous polymer sequentially presents glassy state, high-elastics state, and viscous flow state with an increase in temperature. The tensile test is impossible with the temperature higher than viscous flow temperature. So this paper focuses on the tensile properties of glassy state and high-elastics state of amorphous polymer.

In the glassy state of amorphous polymer, the typical stress vs. strain curves are divided into two parts bounded by the yield point. Before the yield point, the polymer shows elastic properties, and the yield point is the critical point of the elastic stage; after the yield point, the polymer enters the plastic stage. However, the relationship between stress and strain is not completely linear elasticity at the end of the elastic stage. Therefore, the model is divided into three parts as follows: elastic stage, the stage of elastic critical point to yield point, and strain softening stage, which describes the quantitative relationship of stress, strain, and temperature in the glassy state.

The stress-strain relationship is linear in the elastic stage, which is defined as follows [21]:

$$\sigma = E(T) \times \varepsilon; \quad \varepsilon \le 0.25\%, \tag{1}$$

where $\sigma$ and $\varepsilon$ are the stress and strain, respectively. The critical point of elastic stage is 0.25%, referencing the test standard of elastic modulus [22]. $E(T)$ is the elastic modulus relevant to the absolute temperature $T$; in this paper, the relationship of elastic modulus and temperature can be written as

$$E(T) = a_1 \times T^2 + b_1 \times T + c_1, \tag{2}$$

where $a_1$, $b_1$, and $c_1$ are the material constants, respectively.

The trend in the range of elastic critical point to yield point is no longer completely linear, which is described by the power-hardening model [23]:

$$\sigma = A(T)\varepsilon^{B(T)}; \quad 0.25\% < \varepsilon \le \varepsilon_s, \tag{3}$$

where $A(T)$ and $B(T)$ are material parameters considered as the function of the temperature, that is,

$$A(T) \times B(T) = a_2 \times T + b_2, \tag{4}$$

with

$$A(T) = a_3 \times T + b_3, \tag{5}$$

and $\varepsilon_s$ is the yield strain, which is introduced as follows:

$$\varepsilon_s = a_4 \times T^2 + b_4 \times T + c_4, \tag{6}$$

where $a_2$, $a_3$, $a_4$, $b_2$, $b_3$, $b_4$, and $c_4$ are the material constants, respectively.

The relationship of stress and strain in the strain-softening stage is described by the following modified models from the power-hardening model:

$$\sigma = C(T)\varepsilon^{D(T)} + F(T); \quad \varepsilon > \varepsilon_s, \tag{7}$$

where $C(T)$, $D(T)$, and $F(T)$ are the material parameters relevant to the temperature; the quantitative relationships are shown in the following equations:

$$\begin{cases} C(T) = a_5 \times T^2 + b_5 \times T + c_3, \\ F(T) = a_6 \times T^2 + b_6 \times T + c_4, \\ D(T) = \dfrac{a_7 \times T^3 + b_7 \times T^2 + c_5 \times T + d_1}{C(T) \times F(T)}, \end{cases} \tag{8}$$

where $a_5$, $a_6$, $a_7$, $b_5$, $b_6$ $b_7$, $c_3$, $c_4$, $c_5$, and $d_1$ are the material constants, respectively.

The sample exhibits high elasticity as the temperature is higher than the glass transition temperature $T_g$. There is no yield point on the stress vs. strain curves, but a longer platform. This property can be expressed as [21]

$$\sigma = H(T)\varepsilon^{G(T)}, \tag{9}$$

where $H(T) = a_8 \times T^2 + b_8 \times T + c_6$, $G(T) = a_9 \times T^2 + b_9 \times T + c_7$, and $a_8$, $a_9$, $b_8$, $b_9$, $c_6$, and $c_7$ are the material constants.

The model is divided into two parts for describing the quantitative relationship according to material properties at different temperatures. Conclusively, the relationship of temperature and tensile properties of ABS is given as follows:

When $T < T_g$,

$$\sigma = \begin{cases} E(T)\varepsilon; & 0 < \varepsilon \le 0.25\%, \\ A(T)\varepsilon^{B(T)}; & 0.25\% < \varepsilon \le \varepsilon_s, \\ C(T)\varepsilon^{D(T)} + F(T); & \varepsilon > \varepsilon_s. \end{cases} \tag{10}$$

Also, when $T \ge T_g$,

$$\sigma = H(T)\varepsilon^{G(T)}. \tag{11}$$

## 3. Experiments

The tensile samples were made by the amorphous material ABS (XR-401, LG Chemical Information Electronic Materials Co Ltd, Korea), and the tensile specimens were produced by an injection molding machine (HTFX5-MA3800/2250). The processing parameters are shown in Table 1. The tensile tests were performed at different temperatures (40°C, 50°C, 60°C, 70°C, 80°C, 90°C, 100°C, 110°C, 120°C, and 130°C) using a testing machine (Instron-5966, Instron Engineering Corporation, USA), and the tensile rate was 50 mm/min. Further, to verify the correctness of the proposed model, the tensile data of samples at 75°C and 115°C (above and below the glass transition temperature) were carried out for comparison with the data from the proposed model.

Table 1: Processing parameters of ABS in injection molding.

| Processing parameters | Values |
|---|---|
| Injection temperature (°C) | 210 |
| Filling time (s) | 3 |
| Injection pressure (Mpa) | 30 |
| Cooling time (s) | 15 |
| Cooling temperature (°C) | 25 |

## 4. Results and Discussion

*4.1. Parameter Identification.* Tensile properties of ABS vary at different temperatures; in this paper, the temperature of ABS was divided into two parts including below and above the transition temperature. Previous studies had shown that the range of glass transition temperature is 100°C–110°C [24], so the glass transition temperature 105°C was chosen as the boundary between glassy state and high-elastics state of ABS.

*4.1.1. Parameters of Model below the Transition Temperature.* The experimental results of ABS below 105°C are shown in Figure 1. ABS undergoes elastic deformation and plastic deformation in turn as the strain increases. Obviously, the stress gradually increases with the increase of temperature under same strain, and the slope of the stress vs. strain curves decreases correspondingly. The difference of yield stress at 40°C and 90°C is 27.1 MPa, and the tensile properties of ABS are greatly affected by temperature.

The elastic modulus of ABS at different temperature is shown in Table 2, which develops an upward trend with the increase in temperature. This trend is consistent with that of literature [24]. The data were also fitted to obtain the parameters of the model, as shown in Figure 2.

The relationship between elastic modulus and temperature is well described by unary quadratic equation. The value of R-square is 0.99969, which means that the deviation between the fitting curve and experimental data is controlled in a mini confine. The parameters $a_1 = -0.5847$, $b_1 = 360.4405$, and $c_1 = 53035.8534$ of equation (2) were calculated from the fitting curve.

The tensile properties of ABS are obviously affected by temperature due to the viscoelasticity, so the relationship between stress and strain is not linear before yield point. Combining with the test standard, the range of elastic stage is 0–0.25% of strain, in which the relationship between stress and strain is linear. When the strain is in the range of 0.25% to yield strain, the relationship between stress and strain is described by equation (3). The fitting results are shown in Figure 3.

The values of R-square are all greater than 0.93, the largest of which is 0.99398, which means that equation (3) is suitable for describing the relationship between stress and strain in the range of 0.25% to yield strain at different temperatures. The parameters of equation (3) were obtained by the fitting equation, as shown in Table 3.

To explore the relationship between parameters and temperature, the $A$ and $A\times B$ vs. temperature curves are shown in Figure 4. A and A×B decreases monotonously with the increase of temperature, and linear equations were applied to fitting data. $A$ and $A\times B$ of R-square are all larger than 0.97. The acceptable fit results were used for calculating the parameters in equations fd4(4) and (5)fd5. $a_2$, $b_2$, $a_3$, and $b_3$ are −0.3875, 143.7337, −0.3582, and 136.8874, respectively.

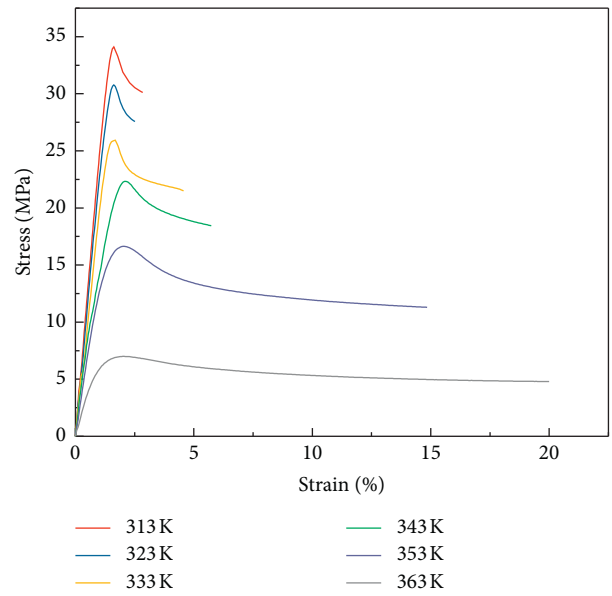


Figure 1: Tensile data of ABS at different temperature (below glass transition temperature).

The yield stress $\varepsilon_s$ was also counted (Figure 5) at different temperatures. The yield stress decreased gradually with the increase of temperature, which decreases from 34.1036 MPa to 6.9964 MPa in the range of 313 K to 363 K. The quadratic functional equation is suitable for the relationship between yield stress and temperature, so the parameters of equation (6) were obtained; $a_4$, $b_4$, and $c_4$ are −0.0063, 3.7049, and −513.8276, respectively.

In the strain softening stage, the fitting results of experimental data are shown in Figure 6. The values of R-square indicated that equation (7) commendably represents the relationship between stress and strain in the strain softening stage. On the basis of the fitting results, the values of $C$, $F$, and $D$ were calculated(Figure 7).

All the parameters of equation (7) were fitted by equation (8), and the parameters of equation (8) were obtained as follows: $a_5 = -0.0078$, $b_5 = 5.0474$, $c_3 = -800.3438$, $a_7 = -0.0474$, $b_7 = 48.2651$, $c_5 = -16316.8925$, $d_1 = 1.8322 \times 10^6$, $a_6 = -0.0065$, $b_6 = 3.8487$, and $c_4 = -540.2021$.

The parameters of the aforementioned model were obtained on the basis of acceptable fitting results. These models reflect the relationship between stress and strain below the glass transition temperature.

*4.1.2. Parameters of the Model above the Transition Temperature.* The tensile properties of ABS at the high-elastics state are different from those at the glassy state,

Table 2: Elastic modulus of ABS at different temperatures.

| Temperature (K) | 313 | 323 | 333 | 343 | 353 | 363 |
|---|---|---|---|---|---|---|
| Elastic modulus, *E (T)* (MPa) | 2499.8156 | 2381.4532 | 2146.4725 | 1823.3530 | 1322.6141 | 761.9812 |

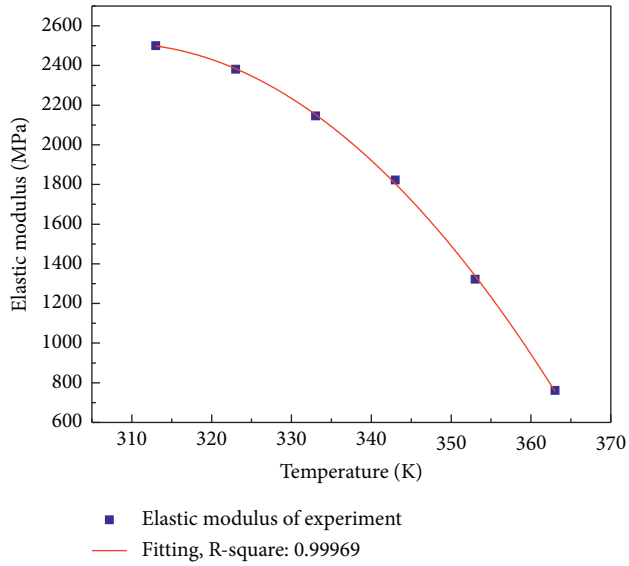


Figure 2: Fitting curve of the elastic modulus at different temperatures.

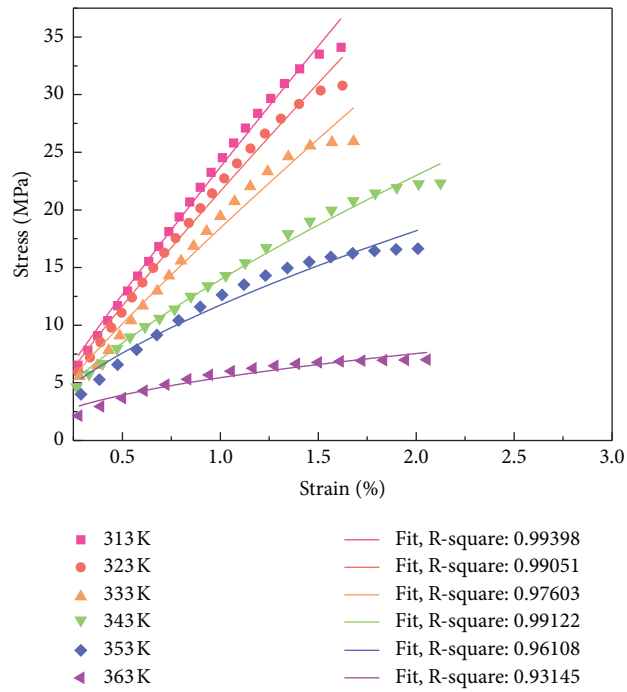


Figure 3: Fitting curve at different temperatures in the range of 0.25% to yield strain.

Table 3: Parameters of equation (3) calculated by the fitting equation.

| Temperature (K) | 313 | 323 | 333 | 343 | 353 | 363 |
|---|---|---|---|---|---|---|
| *A* | 23.7047 | 21.6101 | 18.4354 | 13.9403 | 11.7421 | 5.4501 |
| *B* | 0.9043 | 0.8891 | 0.8613 | 0.7216 | 0.6313 | 0.4689 |
| *A*×*B* | 21.4362 | 19.2135 | 15.8784 | 10.0593 | 7.4128 | 2.5556 |

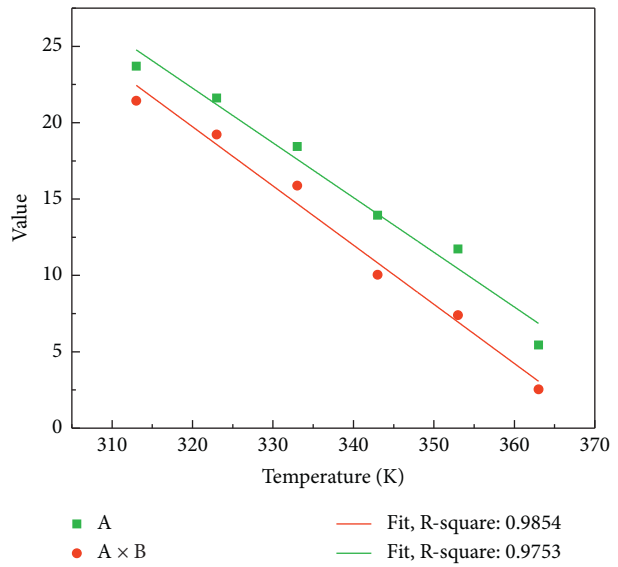


Figure 4: Fitting curves of $A$ and $A \times B$ at different temperatures in equation (3).

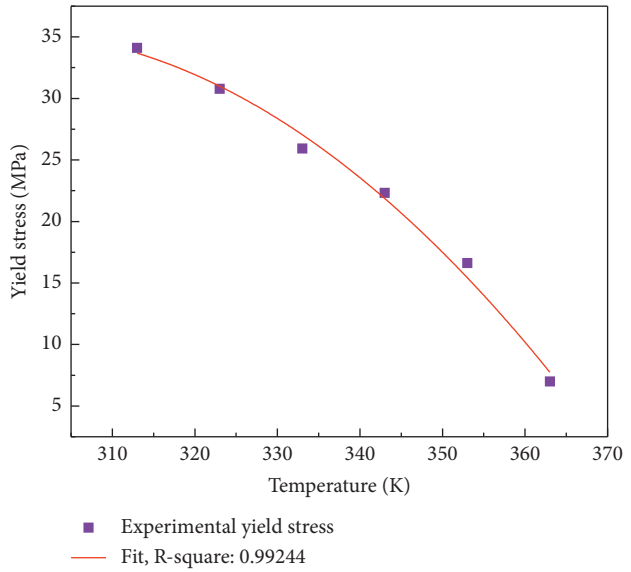


Figure 5: Fitting result of yield stress at different temperatures.

which does not show obvious strain softening and enters directly the plastic stage, as shown in Figure 8.

Equation (9) can be well matched with the experimental results of ABS above the glass transition temperature. The parameters $H$ and $G$ could be calculated on the basis of fitting results, as shown in Figure 9, where $a_8 = 9.0263 \times 10^{-4}$, $b_8 = -0.7160$, $c_6 = 141.9836$, $a_9 = -6.4360 \times 10^{-4}$, $b_9 = 0.5046$, and $c_7 = -98.4584$.

In summary, the parameters of the model were obtained by the fitting in this paper, and the model described the quantitative relationship between stress and strain in a certain temperature range. The quantitative relationship is as follows:When $T < T_g$,

$$\sigma = \begin{cases} \left(-0.5847 \times T^2 + 360.4405 \times T + 530335.8534\right) \times \varepsilon; & 0 < \varepsilon \le 0.25\%, \\ \left(-0.3582 \times T + 136.8874\right) \times \varepsilon^{B(T)}; & 0.25\% < \varepsilon \le \varepsilon_s, \\ \left(-0.0078 \times T^2 + 5.0474 \times T - 800.33438\right) \times \varepsilon^{D(T)} + \left(-0.0065 \times T^2 + 3.8487 \times T - 540.2021\right); & \varepsilon > \varepsilon_s. \end{cases} \quad (12)$$

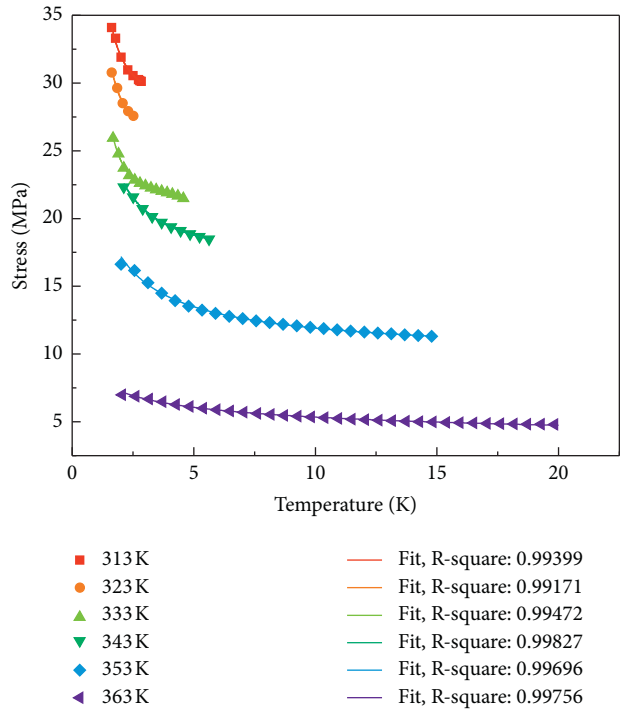


Figure 6: Fitting result of stress in the strain softening stage at different temperatures.

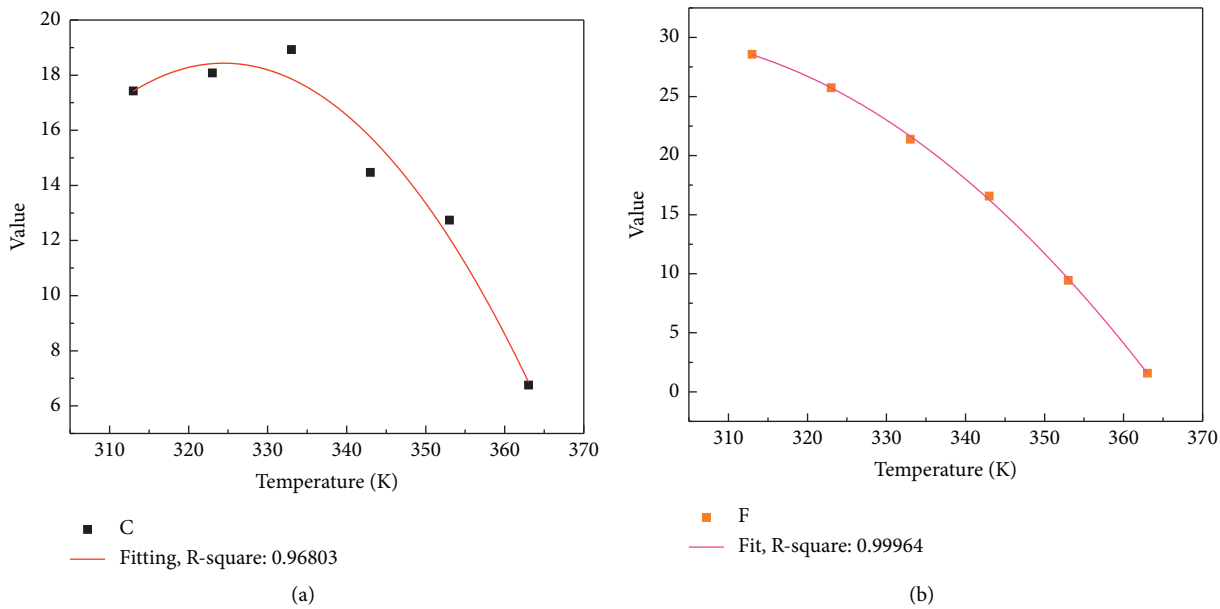


Figure 7: Continued.

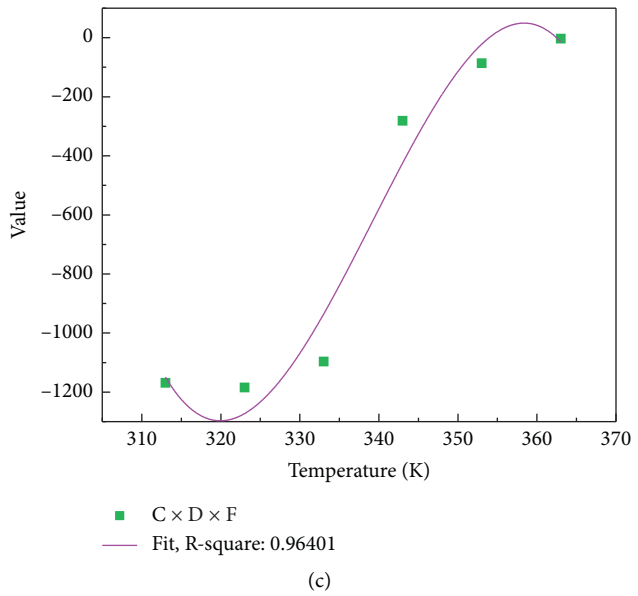


Figure 7: Fitting result of $C$, $F$, and $C \times D \times F$ at different temperatures. (a) $C$, (b) $F$, and (c) $C \times D \times F$.

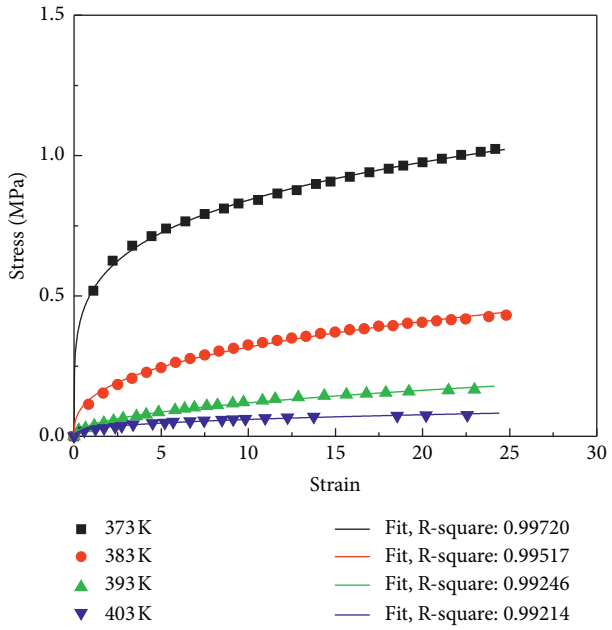


Figure 8: Tensile data of ABS at different temperature (above glass transition temperature).

Also when $T \geq T_g$,

$$\sigma = \left(9.0263 \times 10^{-4} \times T^2 - 0.7160 \times T + 141.9836\right) \times \varepsilon^{G(T)}, \tag{13}$$

where $B(T) = (-0.3875 \times T + 14.7337)/(-0.3572 \times T + 136.8874)$, $\varepsilon_s = -0.0063 \times T^2 + 3.7049 \times T - 513.8276$, $D(T) = (-0.04744 \times T^3 + 48.2651 \times T^2 - 16316.8925 \times T + 1.832\,2 \times 10^6)/((-0.0078 \times T^2 + 5.0474 \times T - 800.33438) \times (-0.065 \times T^2 + 3.8487 \times T - 540.2021))$, and $G(T) = -6.4360 \times 10^{-4} + 0.5046 \times T - 98.4584$.

*4.2. Verification.* To verify the accuracy of the proposed model, the tensile data at 75°C and 115°C were carried out to compare with the data from this model. Combined with the parametric models, the parameters were calculated (Table 4).

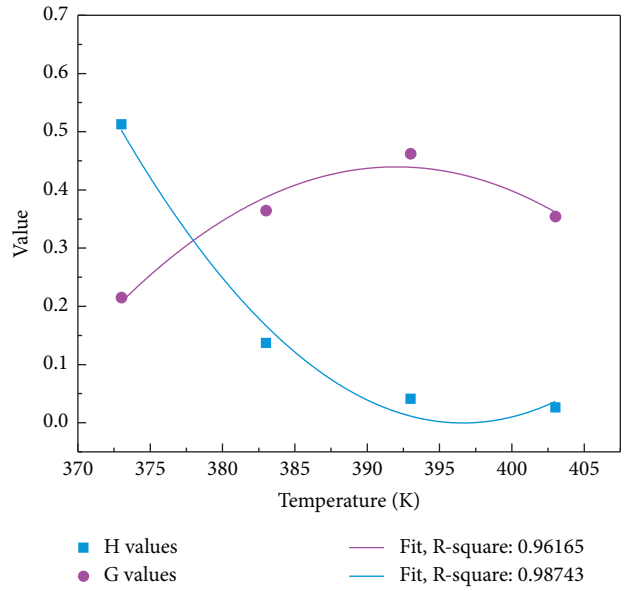


Figure 9: Fitting results of $H$ and $G$ at different temperatures.

Table 4: Parameters of the model at 348 K and 378 K.

| Parameters | | | | | | | | |
|---|---|---|---|---|---|---|---|---|
| 348 K ($T < T_g$) | | | | 388 K ($T \geq T_g$) | | | | |
| $E$ | $A$ | $B$ | $\varepsilon_s$ | $C$ | $D$ | $F$ | $H$ | $G$ |
| 1587.9318 | 12.2338 | 0.7262 | 1.7748 | 13.9484 | −1.8776 | 1.1666 | 0.0681 | 0.4200 |

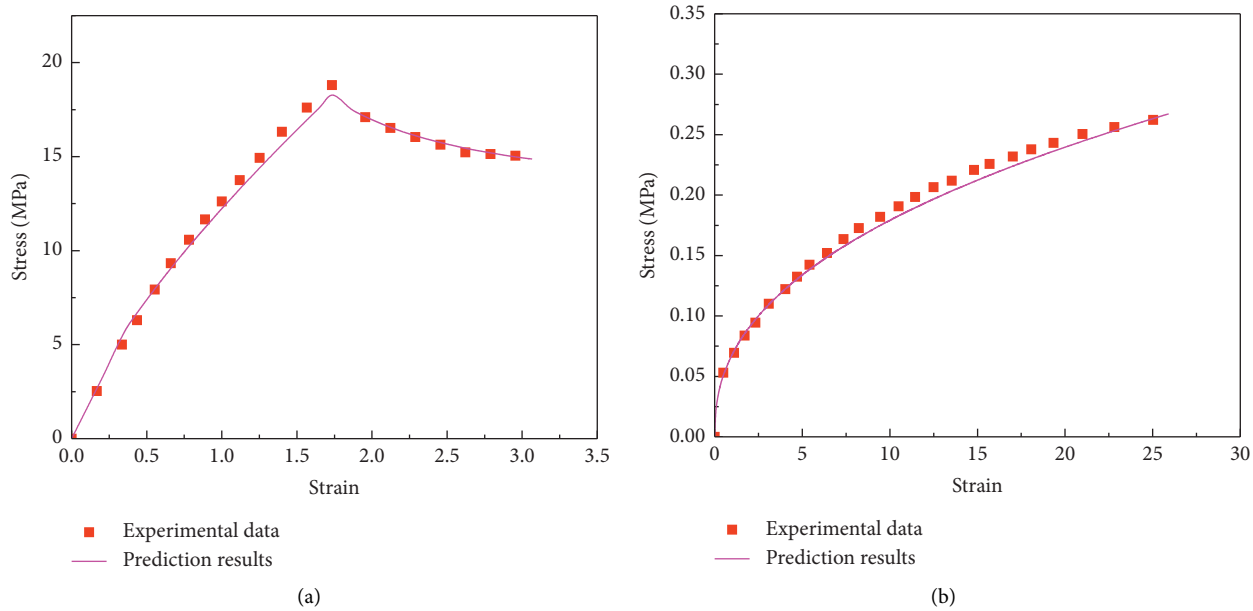


Figure 10: Comparison of experimental data and prediction results at different temperature. (a) 348 K and (b) 388 K.

The comparison of experimental and predicted results at 348 K and 388 K is shown in Figure 10. Clearly, Figure 10 shows that the experimental results agree well with the model predictions by estimated parameters. The small discrepancy can be attributed to material response, which is very complex. Moreover, it is important to emphasize that

the model proposed in this work quantitatively describes the stress-strain relationship of ABS atdifferent temperatures, which reduces the number of experiments.

## 5. Conclusion

In this study, a model is proposed to describe the tensile behavior of ABS at different temperatures. The temperature significantly influences the properties of ABS, and the model is divided into two parts based on the glass transition temperature. The proposed model equations combine mathematical simplicity that facilitates their application to engineering problems with a physically realistic description of the mechanical behavior of ABS. In addition to that, the model was also verified by comparing the experimental data to prediction data from the proposed model. In general, the proposed model accurately describes the tensile behavior of ABS performed at different temperatures, saving time and experimental costs.

## Data Availability

The data used to support the findings of this study are included within the article.

## Conflicts of Interest

The authors declare that they have no conflicts of interest.

## Acknowledgments

This work was supported by the National Natural Science Foundation under Grant nos. 51575491, 51875525, and U1610112 and by the Natural Science Foundation of Zhejiang Province under Grant nos. LY19E050004, LY18E050020, LY20E050020, and LY19E050009.

## References

[1] R. S. Hoy and M. O. Robbins, "Strain hardening of polymer glasses: effect of entanglement density, temperature, and rate," *Journal of Polymer Science Part B Polymer Physics*, vol. 44, no. 24, pp. 3487–3500, 2010.

[2] A. Kozanecka-Szmigiel, J. Antonowicz, D. Szmigiel et al., "On stress-strain responses and photoinduced properties of some azo polymers," *Polymer*, vol. 140, pp. 117–121, 2018.

[3] Y. J. Deng, L. F. Peng, X. M. Lai, M. W. Fu, and Z. Q. Lin, "Constitutive modeling of size effect on deformation behaviors of amorphous polymers in micro-scaled deformation," *International Journal of Plasticity*, vol. 89, pp. 197–222, 2017.

[4] J. Bicerano, N. K. Grant, J. T. Seitz, and K. Pant, "Microstructural model for prediction of stress-strain curves of amorphous and semicrystalline elastomers," *Journal of Polymer Science Part B Polymer Physics*, vol. 35, no. 16, pp. 2715–2739, 2015.

[5] J. Q. Li, T. D. Li, Y. D. Jia et al., "Modeling and characterization of crystallization during rapid heat cycle molding," *Polymer Testing*, vol. 71, 2018.

[6] M. Lei, K. Yu, H. Lu, and H. J. Qi, "Influence of structural relaxation on thermomechanical and shape memory performances of amorphous polymers," *Polymer*, vol. 109, pp. 216–228, 2017.

[7] R. Muthuraj, M. Misra, and A. K. Mohanty, "Biodegradable compatibilized polymer blends for packaging applications: a literature review," *Journal of Applied Polymer Science*, vol. 135, no. 24, 2017.

[8] K. L. Camera, B. Wenning, A. Lal, and C. K. Ober, "Transient materials from thermally-sensitive polycarbonates and polycarbonate nanocomposites," *Polymer*, vol. 101, pp. 59–66, 2016.

[9] X. Rui and T. D. Nguyen, "An effective temperature theory for the nonequilibrium behavior of amorphous polymers," *Journal of the Mechanics & Physics of Solids*, vol. 82, pp. 62–81, 2015.

[10] R. M. Shay and J. M. Caruthers, "A predictive model for the effects of thermal history on the mechanical behavior of amorphous polymers," *Polymer Engineering & Science*, vol. 30, no. 20, pp. 1266–1280, 2010.

[11] T. Yokoyama and K. Nakai, "Determination of high strain-rate compressive stress-strain loops of selected polymers," *Applied Mechanics and Materials*, vol. 24-25, pp. 349–355, 2010.

[12] C. Park, H. Huh, J. Kim, and C. Ahn, "Determination of true stress-true strain curves of polymers at various strain rates using force equilibrium grid method," *Journal of Composite Materials*, vol. 46, no. 17, pp. 2065–2077, 2012.

[13] S. Behzadi and F. R. Jones, "Yielding behavior of model epoxy matrices for fiber reinforced composites: effect of strain rate and temperature," *Journal of Macromolecular Science, Part B*, vol. 44, no. 6, pp. 993–1005, 2005.

[14] J. Richeton, S. Ahzi, K. S. Vecchio, F. C. Jiang, and R. R. Adharapurapu, "Influence of temperature and strain rate on the mechanical behavior of three amorphous polymers: characterization and modeling of the compressive yield stress," *International Journal of Solids and Structures*, vol. 43, no. 7-8, pp. 2318–2335, 2006.

[15] W. Blumenthal, C. Cady, and D. J. Idar, "Influence of temperature and strain rate on the compressive behavior of PMMA and polycarbonate polymers," *AIP Conference Proceedings*, vol. 620, pp. 665–668, 2002.

[16] C. M. Cady, W. R. Blumenthal, G. T. Gray, and D. J. Idar, "Determining the constitutive response of polymeric materials as a function of temperature and strain rate," *Journal de Physique IV*, vol. 110, no. 1, pp. 27–32, 2003.

[17] E. H. M. Han and L. E. Govaert, "Mechanical performance of polymer systems: the relation between structure and properties," *Progress in Polymer Science*, vol. 30, no. 8, pp. 915–938, 2005.

[18] M. M. K. Khan, C. J. Hilado, S. Agarwal, and R. K. Gupta, "Flammability properties of virgin and recycled polycarbonate (PC) and acrylonitrile-butadiene-styrene (ABS) recovered from end-of-life electronics," *Journal of Polymers and the Environment*, vol. 15, no. 3, pp. 188–194, 2007.

[19] C.-Y. Chang, J.-S. Chang, Y.-W. Lin, L. Erdei, and S. Vigneswaran, "Quantification of air stripping and biodegradation of organic removal in acrylonitrile-butadiene-styrene (ABS) industry wastewater during submerged membrane bioreactor operation," *Desalination*, vol. 191, no. 1–3, pp. 162–168, 2006.

[20] Global ABS Market Sales Will Grow by 6% Annually to $38 Billion, http://info.plas.hc360.com/2017/06/261155615858.shtml.

[21] Y. Yao, N. Liao, Z. Miao, and F. Li, "Evaluation of the elastic-plastic properties of SiCN coating system by finite element

simulations," *Journal of the European Ceramic Society*, vol. 37, no. 13, 2017.

[22] J. D. Wang, *General Engineering Plastics Standards Compilation*, Standards Press of China, Beijing, China, 2013.

[23] S. Dul, L. Fambri, and A. Pegoretti, "Fused deposition modeling with ABS-graphene nanocomposites," *Composites Part A: Applied Science and Manufacturing*, vol. 85, pp. 182–191, 2016.

[24] E. Bociaga, "The effect of mold temperature and injection velocity on selected properties of polyethylene moldings," *Polimery*, vol. 45, no. 11/12, pp. 830–836, 2000.